

DEVICES

Longevity decoded: Insights from power consumption analyses into device construction and their clinical implications

Ernest W. Lau MD 

Department of Cardiology, Royal Victoria Hospital, Belfast, Northern Ireland

Correspondence

Ernest Lau MD, Department of Cardiology, Royal Victoria Hospital, Belfast, Northern Ireland BT12 6BA.

Email: ernest.lau@btinternet.com

Abstract

Introduction: The longevity of a cardiac implantable electronic device (CIED) depends on how quickly the powers consumed by the device's functions exhaust its usable battery energy. A mathematical model for CIED power consumptions was developed and validated against longevity data from manufacturers.

Methods: The programmable parameters for the Resonate X4 cardiac resynchronization therapy defibrillators (CRT-Ds) on the Boston Scientific (St. Paul, MN, USA) online longevity calculator were designated as independent terms in the sum for the total power consumption. The reciprocal of longevity was plotted against variations in these terms. Linear and nonlinear regression analyses were used to fit the plots. The power consumed by pacing was theoretically derived and used as the calibrating tool for estimating the powers consumed by other functions and the usable battery energy. The same methodology was applied to the longevity data of other manufacturers' CRT-Ds.

Results: Single chamber 100% pacing at 60 beats/min, 2.5 V, 0.4 ms, 500 Ω consumes \approx 144 J/year. Shock therapy is 45–85% energy efficient. Multichamber pacing modes and maintaining readiness to pace a chamber consume power even if no pacing is delivered. Switching voltage regulation is theoretically more energy efficient than linear voltage regulation for powering pacing.

Conclusions: The powers consumed by therapy functions are dictated by the patient's clinical needs, but healthcare professionals can extend device longevity by switching off dormant functions and simplifying the pacing mode. Choosing a device model with large usable battery energy, low background power, and energy efficient pacing and shock therapy for implantation will increase the probability of a long service lifespan.

KEYWORDS

background power, linear regulation, longevity, power consumption, regression analyses, switching regulation, usable battery energy, voltage multiplication-division

1 | INTRODUCTION

The longevity of cardiac implantable electronic devices (CIEDs) should be an important if not the primary performance attribute in model choice, as battery depletion is the dominant cause of device replacement,¹ which entails not only fiscal cost² but also risk of infection and lead failure.^{3–6} The longevity quoted by manufacturers

for their latest generation of device models are inevitably projections (typically based on nonuniform settings)^{7,8} and have historically turned out to be overestimates in clinical practice, even after correction for use conditions.^{9–11} The observed longevity reported in single/multicenter studies, registries, and product performance reports (PPRs) can only pertain to previous generations of device models, which have become technologically obsolete and may no longer be

available for new implantation by the time significant clinical experience has accrued.^{12,13} Confronted with a bewildering array of conflicting claims and estimates, implanters cannot readily base model choice on longevity, which is an especially important clinical concern for implantable cardioverter-defibrillators (ICDs) and cardiac resynchronization therapy defibrillators (CRT-Ds).

Boston Scientific (BSc; St. Paul, MN, USA) is the first CIED manufacturer to provide an open access online device longevity calculator. Data from the calculator can be used to deduce the functional (and structural) components of BSc CIEDs and their power consumptions. That knowledge was used to develop a mathematical model that produced reasonably accurate longevity projections for any arbitrary settings. The same methodology was also successfully applied to device models by other CIED manufacturers despite many fewer longevity projections were listed in the publicly available information sources. Even from the limited information released by manufacturers, valuable insights can be gained into the construction and power consumptions of their devices to guide device selection and programming.

2 | METHODS

See Table 1 for a list of the symbols and abbreviations.

2.1 | Relationships between longevity, battery energy, and power consumptions

If a CIED has usable battery energy W° , its longevity in service t° is given by:

$$t^\circ = \frac{W^\circ}{P^\circ} \quad (1a)$$

$$P^\circ = \sum_n P_n, \quad (1b)$$

where P° is the sum of the average powers P_n 's consumed by the different functions/components (assumed to be independent and additive). While some functions are performed continuously (e.g., running the device's operating system, heart rhythm monitoring), other functions are performed periodically (e.g., remote transmission, high-voltage capacitor reformation, battery conditioning), intermittently (e.g., pacing), or sporadically (e.g., shocks).

2.2 | Pacing impulse energy

The energy of a pacing impulse W_p (in joule, J) of duration τ_p (in second) depends on whether switching regulation (SR) or linear regulation (LR) is used to produce the (peak) output amplitude V_p (in volt, V) (see Appendix A)¹⁴:

$$\begin{aligned} \langle W_p \rangle_{SR} &= \frac{C_p V_p^2}{2} \left[1 - \exp\left(-\frac{2}{C_p} \cdot \frac{\tau_p}{Z_p + \alpha_p}\right) \right] \\ &\approx \frac{V_p^2 \tau_p}{Z_p + \alpha_p} \left(1 - \frac{1}{C_p} \cdot \frac{\tau_p}{Z_p + \alpha_p} \right) \approx \frac{V_p^2 \tau_p}{Z_p + \alpha_p}, \end{aligned} \quad (2)$$

TABLE 1 List of symbols and abbreviations

Symbol/abbreviation	Meaning
CIED	Cardiac implantable electronic device
ICD	Implantable cardioverter defibrillator
CRT-D	Cardiac resynchronization therapy defibrillator
SR	Switching (voltage) regulation/regulator
LR	Linear (voltage) regulation/regulator
W°	Usable battery energy
t°	Device longevity
P°	Total device power consumption
P_n	Power consumed by a function
P_{00}	Device background power consumption
$W_p (W_k)$	Pacing impulse energy (for a particular cardiac chamber)
$\langle W_p \rangle_{SR}$	Pacing impulse energy (switching voltage regulation)
$\langle W_p \rangle_{LR}$	Pacing impulse energy (linear voltage regulation)
f_p	Pacing frequency (base rate)
$\%_p (\%_k)$	Percentage of pacing (for a particular cardiac chamber)
V_b	Battery voltage
$V_p (V_k)$	Peak pacing output amplitude (for a particular cardiac chamber)
$V_C (V_{Ck})$	Peak pacing capacitor voltage (for a particular cardiac chamber)
$\tau_p (\tau_k)$	Pacing pulse width (for a particular cardiac chamber)
Z_p (or Z_k)	Pacing load impedance (for a particular cardiac chamber)
$\alpha_p (\alpha_k)$	Pacing internal impedance (for a particular cardiac chamber)
$C_p (C_k)$	Pacing capacitance (for a particular cardiac chamber)
$\eta_p (\eta_k)$	Pacing energy efficiency (for a particular cardiac chamber)
$P_p (P_{1k})$	Average pacing power (for a particular cardiac chamber)
W_s	Shock energy
f_s	Shock frequency
spyr	Shocks per year
η_s	Shock energy efficiency
P_s	Average shock therapy power
m	Slope of linear regression line
x_0	Horizontal intercept of linear regression line
y_0	Vertical intercept of linear regression line
λ	Scale factor for variable in linear regression against $1/t^\circ$
k	An integer referring to a particular cardiac chamber

$$\begin{aligned} \langle W_p \rangle_{LR} &= \frac{C_p V_C^2}{2} \left[1 - \exp\left(-\frac{2}{C_p} \cdot \frac{V_p}{V_C} \cdot \frac{\tau_p}{Z_p + \alpha_p}\right) \right] \\ &\approx \frac{V_C V_p \tau_p}{Z_p + \alpha_p} \left(1 - \frac{1}{C_p} \cdot \frac{V_p}{V_C} \cdot \frac{\tau_p}{Z_p + \alpha_p} \right) \approx \frac{V_C V_p \tau_p}{Z_p + \alpha_p}, \end{aligned} \quad (3)$$

where Z_p (in ohm, Ω) is the load impedance, α_p (in Ω) is the internal resistance, C_p (in farad, F) is the pacing capacitance, and V_C (in V) is the (peak) capacitor voltage. (V_C may be below, equal to, or above the device's battery voltage V_b).

α_p and C_p can be estimated from limited longevity data (see Appendices B and E), which then allows W_p to be calculated for different pacing parameters. W_p can be used as an "energy unit" to estimate the powers consumed by other functions and the usable battery energy W° (see below). In clinical practice, τ_p is typically expressed in ms. Pacing capacitance C_p is thus more conveniently expressed in millifarad (mF) rather than the more commonly used microfarad (μ F) as the term $\tau_p/C_p(Z_p + \alpha_p)$ will automatically be a dimensionless value without scaling. With the same convention on units, the terms $C_p V_p^2$, $C_p V_C^2$, $V_p^2 \tau_p / (Z_p + \alpha_p)$, and $V_C V_p \tau_p / (Z_p + \alpha_p)$ will have the unit of millijoule (mJ). Equation (2)/(3) allows the pacing impulse energy W_p to be calculated exponentially, quadratically, or linearly.

2.3 | Pacing power consumption

For pacing frequency (base rate) f_p and percentage $\%_p$, the power consumed P_p is:

$$P_p = \frac{f_p \%_p}{\eta_p} W_p = \frac{f_p \%_p}{\eta_p} W_p (V_p, \tau_p, Z_p, \alpha_p, C_p, V_C), \quad (4)$$

where $\eta_p > 0$ is the energy efficiency of pacing after allowing for the internal resistance α_p .

In clinical practice, f_p is typically expressed in beats/min, whereas the reciprocal of device longevity $1/t^\circ$ is in year⁻¹ (yr⁻¹).

$$1 \text{ yr} = 365 \times 24 \times 60 \text{ min} = 525600 \text{ min} \Rightarrow \frac{1}{\text{min}} = \frac{525600}{\text{yr}}$$

$$1 \text{ beats/min} \cdot \% = \frac{1}{\text{min}} \cdot \frac{1}{100} = \frac{525600}{\text{yr}} \cdot \frac{1}{100} = 5256 \text{ yr}^{-1}.$$

With the units used clinically, W_p has the unit of mJ. P_p thus has the unit of:

$$5256 \text{ yr}^{-1} \times 10^{-3} \text{ J} = 5.256 \text{ J/yr},$$

$$1 \text{ J/yr} = \frac{1 \text{ J}}{365 \times 24 \times 60 \times 60 \text{ s}} = 3.17 \times 10^{-8} \text{ J s}^{-1} = 0.0317 \mu\text{W}.$$

Battery capacity is typically quoted in ampere-hour (A·h). Assuming an average voltage of 2.9 V for a lithium anode primary battery used to power CIEDs:

$$1 \text{ A} \cdot \text{h} @ 2.9 \text{ V} = 3600 \times 12.9 \text{ J} = 10440 \text{ J}.$$

2.4 | Shock therapy power consumption

The (average) power consumed by (sporadic) shock therapy P_s is:

$$P_s = f_s \frac{W_s}{\eta_s}, \quad (5)$$

where W_s is the energy (in J) stored on (generally not completely delivered by) the high-voltage capacitor for each shock, f_s is the shock frequency (in shocks per year, or spyr), and $\eta_s > 0$ is the shock energy efficiency. With these units, P_s has the unit of J/yr.

TABLE 2 Power consuming functions (components) of a CRT-D model

Function (component)	Symbol	Formula	$\Delta(1/t^\circ)$ for Resonate X4
Running the operating system	P_0	P_0	0.058
Pacing $k = 0$ atrial $= 1$ RV $= 2$ LV $= 3$ LV _b	P_1	$P_{1k} = \frac{f_p \%_k}{\eta_k} W_k$	variable
Shock therapy	P_2	$P_2 = f_s \frac{W_s}{\eta_s}$	1spyr = 0.0021 for $f_s \leq 4$ 1spyr = 0.0042 for $f_s > 4$
Brady mode $k = 0$ OOO (off) $= 1$ VVI(R) $= 2$ AAI(R) $= 3$ VDD(R) $= 4$ DDI(R) $= 5$ DDD(R)	P_3	$\sum_{k=0}^5 P_{3k} \mathbf{1}_{3k}$	$P_{30} = 0$ $P_{31} = 0.0037$ $P_{32} = 0.0037$ $P_{33} = 0.0057$ $P_{34} = 0.0065$ $P_{35} = 0.0067$
Ventricular chambers paced $k = 0$ no V; $= 1$ RV only $= 2$ BiV $= 3$ LV only	P_4	$\sum_{k=0}^2 P_{4k} \mathbf{1}_{4k}$	$P_{40} = 0$ $P_{41} = 0.001$ $P_{42} = 0.004$ $P_{43} = 0.001$
Multisite pacing	P_5	$P_{50} \mathbf{1}_{50}$	$P_5 = 0.0012$
Remote monitoring	P_6	$P_{60} \mathbf{1}_{60}$	$P_6 = 0.0033$
Minute ventilation	P_7	$P_{70} \mathbf{1}_{70}$	$P_7 = 0.003$
Heart failure sensor suite	P_8	$P_{80} \mathbf{1}_{80}$	$P_8 = 0.0006$
SonR	P_9	$P_{90} \mathbf{1}_{90}$	–

Note: A = atrial; CRT-D = cardiac resynchronization therapy defibrillator; LV = left ventricular; RV = right ventricular. Turning the brady mode off and pacing no ventricular chamber are assumed to consume no power (i.e., $P_{30} = 0$ and $P_{40} = 0$). Figures in the last column pertain only to the Resonate X4 G447 CRT-D. (See Table 1 for meanings of the symbols and notations).

2.5 | Other power consumptions

As the CRT-D has the largest set of programmable functions for CIEDs and the BSc online longevity calculator was the most accessible tool for longevity projection study, the Resonate X4 G447 was used to build the basic list of power consumptions P_n 's (Table 2). Functions common to all CIEDs were assigned lower indices in the list. Functions unique to particular device models (e.g., minute ventilation, heart failure suite, SonR) were assigned higher indices. The list so generated should thus be general enough to be applicable to most CIED models.

Substituting Eqs. (4) and (5) into Eq. (1b):

$$P^\circ = P_0 + f_p \sum_{k=0}^3 \frac{\%_k}{\eta_k} W_k + f_s \frac{W_s}{\eta_s} + \sum_{n \geq 3} \sum_{k=0}^n P_{nk} \mathbf{1}_{nk}. \quad (6)$$

P_0 is the minimum power needed to operate the device. The P_{1k} 's are the powers consumed by pacing the atrium (A), right ventricle (RV), left ventricle (LV), and a second LV site (LV_b). P_2 is the power consumed

by shock therapy. The P_{3k} 's are the powers consumed by the pacing modes. The P_{4k} 's are the powers consumed by maintaining readiness to pace the ventricular chambers. (P_{40} is not available in the BSc online longevity calculator but was assumed if pacing the RV, LV, or both makes no difference to $1/t^\circ$, as for the OOO or AAI(R) mode.) The P_{n0} 's ($n \geq 5$) are single-option binary ("on-off") functions ($j_n = 0$ in Eq. (6)). The $\mathbf{1}_{nk}$'s ($n \geq 3$) are indicator functions that take the value of 0 or 1 depending on whether the corresponding functions are off or on.

2.6 | Estimation of usable battery energy and power consumptions

Inverting Eq. (1a) and substituting Eqs. (4) and (6) into Eq. (1b) give:

$$\frac{1}{t^\circ} = \frac{1}{W^\circ} \left(P_0 + f_p \sum_{k=0}^3 \frac{\%_k}{\eta_k} W_k (V_k, \tau_k, Z_k, \alpha_k, C_k, V_{Ck}) + f_s \frac{W_s}{\eta_s} + \sum_{n \geq 3} \sum_{k=0}^{j_n} P_{nk} \mathbf{1}_{nk} \right). \quad (7)$$

Equation (7) is a linear equation in multiple variables (which may be derivatives of one or more parameters). Changing only one of these variables x at a time and lumping the terms containing all the other constant variables into a background power P_{00} , Eq. (7) becomes:

$$\frac{1}{t^\circ} = \frac{1}{W^\circ} (P_{00} + \lambda x). \quad (8)$$

By Eq. (8), a plot of $1/t^\circ$ against x will be a straight line of slope $m = \lambda/W^\circ$, vertical intercept $y_0 = P_{00}/W^\circ$, and horizontal intercept $x_0 = -P_{00}/\lambda$. The values of m , y_0 , and x_0 can be readily estimated with linear regression from any suitable data set. Once these regression coefficients are known, other variables in Eq. (8) can be estimated:

$$\text{If } \lambda \text{ is known: } \quad W^\circ = \lambda/m \quad (9a)$$

$$P_{00} = -\lambda x_0 \quad (9b)$$

$$\text{If } W^\circ \text{ is known: } \quad \lambda = mW^\circ \quad (9c)$$

$$P_{00} = y_0 W^\circ. \quad (9d)$$

A pacing power P_{1k} depends on nine variables: f_p , $\%_k$, V_k , τ_k , Z_k , η_k , α_k , C_k , V_{Ck} (Eq. (4)). The first five variables can change significantly in clinical use, whereas the last four may be regarded as fixed and their values estimated from available longevity data (see Appendices B and E). From Eqs. (2)/(3) and (7), if x is P_{1k} , f_p , $\%_k$, V_k (or V_k^2), it will have a linear relationship with $1/t^\circ$. The value of λ can be calculated from Eqs. (2)/(3) and (4). This means W° and P_{00} can be estimated from the linear regression coefficients with Eqs. (9a) and (9b). Once W° has been estimated for a device, it can be used to estimate the λ and P_{00} for a different regression line (from another variable-background power pair) with Eqs. (9c) and (9d).

From Eq. (7), f_s has a linear relationship with $1/t^\circ$ with $\lambda = W_s/\eta_s$. Since W_s (generally assumed to be the maximum shock energy

possible) is always supplied by the manufacturer, if W° is known, from Eq. (9c):

$$\lambda = \frac{W_s}{\eta_s} = mW^\circ \Rightarrow \eta_s = \frac{W_s}{mW^\circ}. \quad (10)$$

Shock energy efficiency can also be estimated by establishing the equivalence (in terms of impact on longevity) between shock and pacing powers. If a rise in shock frequency Δf_s has the same impact on device longevity as a rise in pacing power ΔP_p , then:

$$\Delta \left(\frac{1}{t^\circ} \right) = \frac{\Delta P_s}{W^\circ} = \frac{\Delta P_p}{W^\circ} \Rightarrow \Delta P_s = \Delta f_s \frac{W_s}{\eta_s} = \Delta P_p \Rightarrow \eta_s = \frac{\Delta f_s \cdot W_s}{\Delta P_p}. \quad (11)$$

If $x = \mathbf{1}_{nk}$, then $\lambda = P_{nk}$ and:

$$\frac{P_{nk}}{W^\circ} = \frac{1}{t^\circ} (\mathbf{1}_{nk} = 1) - \frac{1}{t^\circ} (\mathbf{1}_{nk} = 0) = \Delta \left(\frac{1}{t^\circ} \right)_{nk}. \quad (12)$$

Equation (12) means the power of a programmable function P_{nk} can be estimated from the difference in the reciprocal of longevity between switching the function on and off, and this difference is well-defined and independent of the background power P_{00} (i.e., $\Delta(1/t^\circ)_{nk}$ will not have different values depending on P_{00}). If W° is constant for a device model, $\Delta(1/t^\circ)_{nk}$ can be used as a surrogate measure of P_{nk} .

2.7 | Validation of mathematical model

To assess the powers consumed by pacing, one out of five parameters (f_p , $\%_k$, V_k , τ_k , Z_k) for one or more cardiac chambers was altered at a time. The plot of $1/t^\circ$ against the varying parameter or its derivative (e.g., V_k^2 , $1/Z_k$, τ_k/Z_k) was inspected for a possible algebraic (linear, quadratic, or exponential) relationship, and regression analysis was performed whenever a reasonable fit could be achieved. The regression coefficients were used to estimate the internal resistance α_k and pacing capacitance C_k (see Appendices B and E), which would in turn be used to calculate the pacing power P_p by Eqs. (2)/(3) and (4). Once P_p is known, the other terms in Eq. (7) were calculated using Eqs. (8)–(12).

2.8 | Numerical analyses

All regression analyses were performed by the least-square criterion with a statistical package (Prism, GraphPad Software, San Diego, CA, USA).

2.9 | Device models and data sources for longevity and power consumption analyses

Only CRT-D models were analyzed. For BSc, the Resonate X4 G447 was chosen (data source: online longevity calculator). For Abbott (Abt, formerly St. Jude Medical, Sylmar, CA, USA), the Quadra Assura MP model CD3369-40Q was chosen (data source: PPR 2018, 1st edition; manufacturer's technical support). For Microport (Mcp, formerly LivaNova, Clamart, France), the Platinum 4LV SonR model 1844 was chosen (data source: online device longevity stimulator, <http://www.cardiacdevice longevity.com/longevity/>, manufacturer's technical

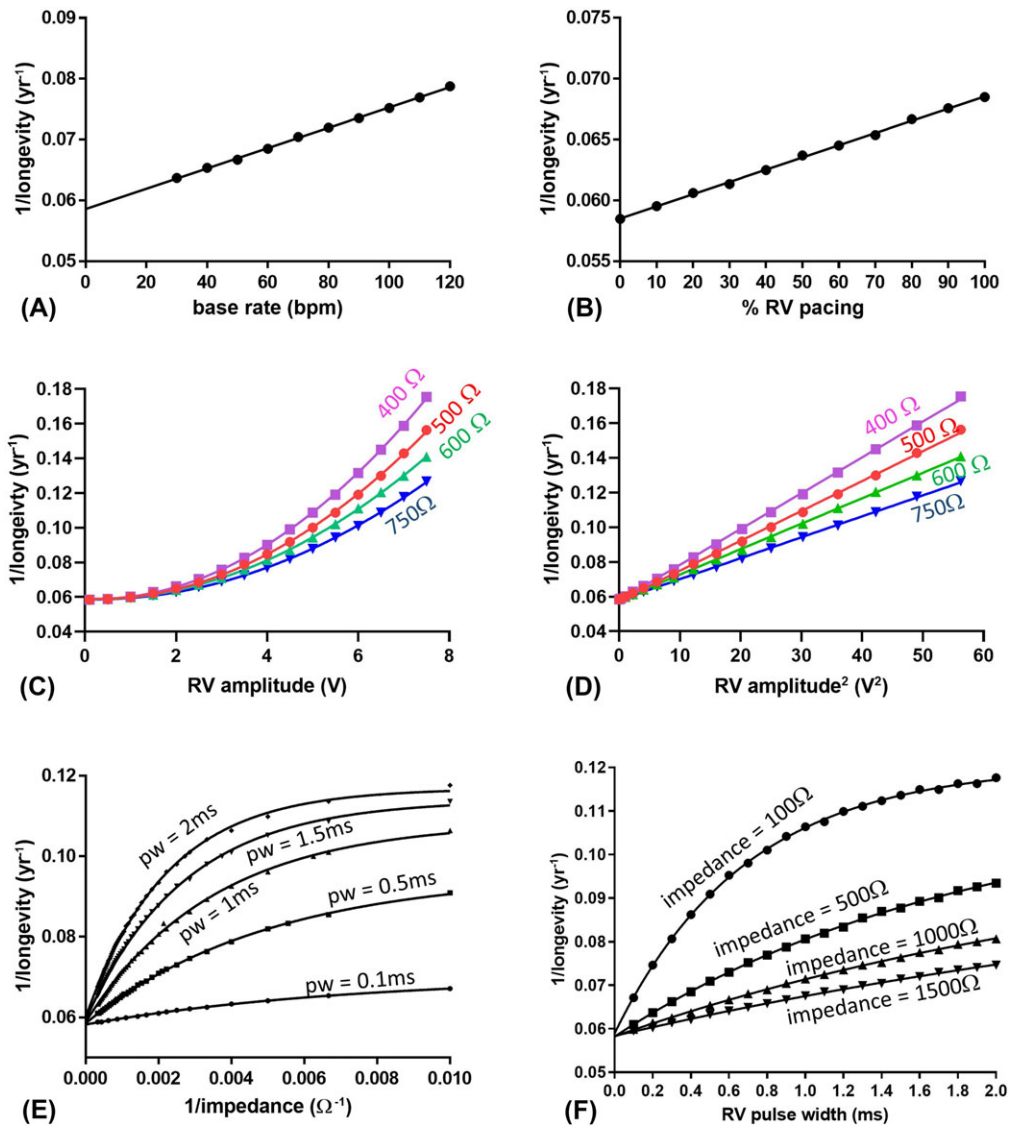


FIGURE 1 Effects of RV pacing parameters on Resonate X4 longevity. Plots produced with figures obtained from the online longevity calculator provided by Boston Scientific for the Resonate X4 G447 CRT-D. The reciprocal of longevity is linearly related to the base rate (A) and percentage (B) of pacing, and the square of the output amplitude (C) and (D). The reciprocal of longevity appears to be related to the reciprocal of impedance (E) and pulse width (pw) (F) through an inverted negative exponential rise to a plateau, and the two factors affect each other’s relationship. RV = right ventricular [Color figure can be viewed at wileyonlinelibrary.com]

support). For Biotronik (Btk, Berlin, Germany), the Intica 7 HF-T (QP) was chosen (data: manual). For Medtronic (Mdt, Minneapolis, MN, USA), the Viva Quad XT model DTBA1QQ was chosen (data source: manual; a previous publication¹⁵).

3 | RESULTS

3.1 | SR for pacing

The Resonate X4 was set to VVIR (P_{31}) and RV-only pacing (P_{41}), with no shock therapy and all nonessential functions off on the BSc online longevity calculator. The default values were: $f_p = 60$ beats/min; $\%_1 = 100\%$; $V_1 = 2.5$ V; $\tau_1 = 0.4$ ms; $Z_1 = 500 \Omega$. The $1/t^{\circ} - f_p$ and $1/t^{\circ} - \%_1$ plots are straight lines (Figures 1A and

B). The $1/t^{\circ} - V_1$ plot is a parabola (Figure 1C) but the $1/t^{\circ} - V_1^2$ plot is a straight line (Figure 1D), which suggests SR (see Appendices A and B).

The $1/t^{\circ} - 1/Z_1$ and $1/t^{\circ} - \tau_1$ plots are a series of convex upward curves for different values of the other variable (Figures 1E and F). When $1/t^{\circ}$ is plotted against τ_1/Z_1 , both sets of curves become better but still not perfectly aligned (Figures 2A and B). However, the “iso-longevity” curves of (τ_1, Z_1) pairs giving rise to the same longevity (with linear interpolation between adjacent data points when the exact longevity figure was not given by the online calculator) are straight lines (Figure 2C), which suggests t° is dependent on (τ_1, Z_1) only through their ratio $\tau_1/(Z_1 + \alpha_1)$, where $\alpha_1 \approx 60 \Omega$ corrects for the negative intercept on the Z_1 axis by the iso-longevity lines (Figure 2C). When $1/t^{\circ}$ is plotted against $\tau_1/(Z_1 + \alpha_1)$, both sets of curves become perfectly aligned and in fact overlapping (Figures 2D and E). When

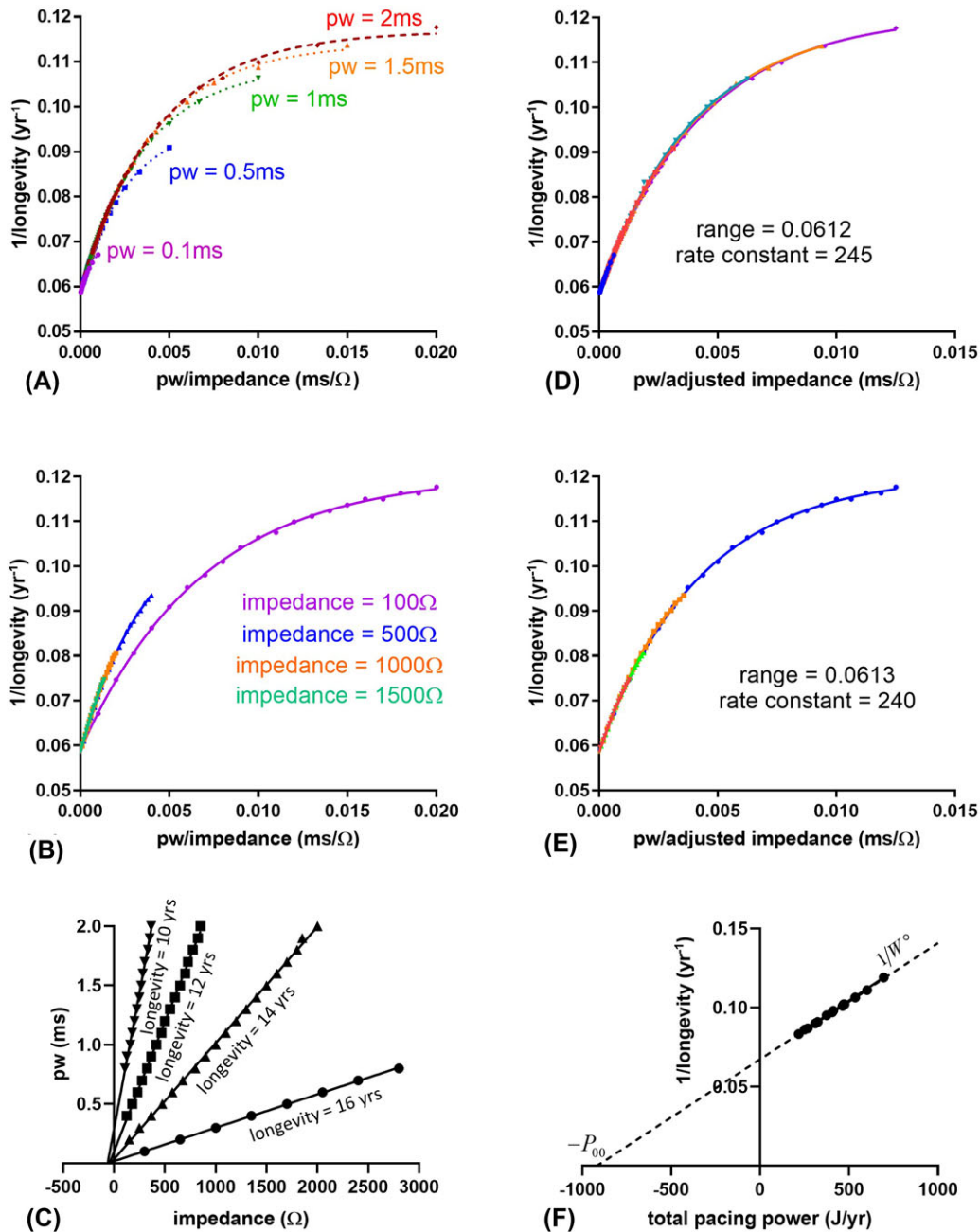


FIGURE 2 Effects of the pw: impedance (with or without adjustment for internal resistance) ratio on Resonate X4 longevity. (A) and (B) For a fixed pacing amplitude, the pw: impedance ratio does not consistently predict the reciprocal of longevity. (C) Iso-longevity curves suggest a correction term, an internal resistance, needs to be added to the load impedance to give an adjusted impedance. (D) and (E) The pw: adjusted impedance ratio consistently predicts the reciprocal of longevity. (F) The plot of the reciprocal of longevity against the total pacing power for the settings in the Viva Quad XT manual incorporating the estimated internal resistance and pacing capacitance is a straight line. The slope of the line is the reciprocal of the usable battery energy $1/W^\circ$. The horizontal intercept is the negative value of the background power P_{00} . pw = pulse width [Color figure can be viewed at wileyonlinelibrary.com]

the two sets of curves were regressed for an exponential model (general equation $y = y_0 + (y_1 - y_0)(1 - e^{-\kappa x})$), the vertical intercepts y_0 (0.05852 and 0.05874), vertical spans $y_1 - y_0$ (0.0612 and 0.0613), and rate constants κ (244.5 and 239.8) are similar. From Eq. (2):

$$\frac{2}{C_1} = \kappa = 240 \Rightarrow C_1 = 0.008 \text{ mF.}$$

Figures 2C–E give a graphical way of estimating internal resistance α_1 and capacitance C_1 , but their values can also be estimated

analytically (see Appendix B). For $\alpha_1 = 100 \Omega$ and $C_1 = 0.01 \text{ mF}$, $\langle W_p \rangle_{SR} = 0.0039 \text{ mJ}$ (see Appendix A). By Eq. (4), assuming $\eta_1 = 0.85$:

$$P_p = f_p \%_p \frac{W_p}{\eta_p} = 5.256 \times 60 \times 100 \times \frac{0.0039}{0.85} \text{ J/yr} = 144 \text{ J/yr.}$$

For the variables with a linear relationship with $1/t^\circ$ (f_p , $\%_1$, and V_1^2 , Figures 1A, B, and D), the slope m and horizontal intercept x_0 of the regression line were used to estimate W° and P_{00} (Table 3). Using

TABLE 3 Linear regression parameters and resulting estimates of usable battery energy and background power for Resonate X4 CRTD programmed to VVI(R) right ventricular (RV) pacing

Variable	Base rate f_p (beats/min)	% RV pacing $\%_1$ (%)	RV amplitude ² V_1^2 (V ²)	Pacing power $P_1 = \sum_{k=0}^2 P_{1k}$ (J/yr)
Corresponding graph	Figure 1a	Figure 1b	Figure 1d	Figure 2f
Slope m	0.000167	0.0001004	0.001721	0.00007343
Horizontal intercept x_0	-350.7	-582.6	-33.55	-917.8
Scale factor λ	$P_p/60$	$P_p/100$	$P_p/2.5^2$	1
Usable battery energy $W^\circ = \lambda/m$	14401 J (≈ 1.38 A·h)	14373 J (≈ 1.38 A·h)	13415 J (≈ 1.29 A·h)	13619 J (≈ 1.30 A·h)
Background power* $P_{00} = -\lambda x_0$	843 J/yr (26.7 μ W)	841 J/yr (26.6 μ W)	775 J/yr (24.6 μ W)	918 J/yr (29.1 μ W)

Note: $P_p = 144$ J/yr for $F_p = 60$ beats/min; $\%_1 = 100\%$; $\eta_1 = 0.85$; $\tau_1 = 0.4$ ms; $Z_1 = 500$ Ω ; $\alpha_1 = 100$ Ω ; $C_1 = 0.01$ mF.

*For the first 3 columns, $P_{00} = P_0 + P_{31} + P_{41}$. For the last column, $P_{00} = P_0 + P_{35} + P_{42} + P_{60}$.

Comparing the background power for the first 3 columns and the last column, remote monitoring consumes ≈ 80 J/yr.

(For explanation of symbols and notations, see Tables 1 and 2.)

the same values for the internal resistance, capacitance, and energy efficiency for all three pacing channels, the total pacing power $P_1 = \sum_{k=0}^2 P_{1k}$ for the settings in the Viva Quad XT CRT-D manual (which involve simultaneous changes in the amplitude and impedance of all three pacing channels) was calculated (see Appendix C). The $1/t^\circ - P_1$ plot is a straight line (Figure 2F), validating Eqs. (2) and (4) used in P_1 's calculation (Table 3).

3.2 | LR for pacing

The longevity data supplied by the manufacturer of the Quadra Assura MP assumed 100% A, RV and LV pacing at 60 beats/min, 3 spyr, daily alert, and remote follow-up every 3 months. A and RV pacing were fixed at 2.5 V, 0.5 ms, and 500 Ω . The LV pacing parameters varied: 0.5–7.5 V for amplitude V_2 , 0.5–1.5 ms for pulse width τ_2 , and 400–1500 Ω for load impedance Z_2 .

Keeping τ_2 and Z_2 fixed, the $1/t^\circ - V_2$ plot comprises three rising steepening straight line segments separated by widening abrupt jumps at $V_2 = 2.5, 5,$ and 7.5 V, with a common $1/t^\circ$ intercept and slopes proportional to the V_2 value at their upper ends (i.e., 2.5, 5, and 7.5, Figure 3A). Quadratic regression for the upper ends of the three straight line segments produces a parabola that also shares their common $1/t^\circ$ intercept. The $1/t^\circ - V_2^2$ plot comprises three rising flattening convex curve segments separated by widening abrupt jumps and whose upper ends lie on a straight line (Figure 3B). The pattern is consistent with LR with peak pacing capacitor voltage $V_{C2} = 2.5, 5,$ and 7.5 V (see Appendices A and B). When $V_C = V_p$, LR impacts longevity like SR (Figure 1D).

Keeping V_2 and Z_2 fixed, the $1/t^\circ - \tau_2$ plot appears to be a straight line but has only four points (Figure 3C). Keeping τ_2 fixed at 1.5 ms (chosen for accentuation of any deviation from linearity), the $1/t^\circ - 1/Z_2$ plot is a series of convex upward curves with curvature positively correlated with V_2 (Figure 3D). There were not enough data points to conduct iso-longevity analysis as in Figure 2C. Instead, the slopes of the linear $1/t^\circ - V_2$ plot (Figure 3A) for different values of Z_2 were used to estimate the internal resistance α_2 (≈ 120 Ω) (see Appendix B). The $1/t^\circ - \tau_2/(Z_2 + \alpha_2)$ plot is still a series of convex upward curves but has many more data points on each due to the larger number of

($\tau_2, Z_2 + \alpha_2$) combinations (Figure 3E). By modeling the $1/t^\circ - \tau_2/(Z_2 + \alpha_2)$ plot as a parabola, the capacitance C_2 (≈ 0.01 mF) was estimated (see Appendix B). These estimates of α_2 and C_2 allow the total pacing power $P_1 = \sum_{k=0}^2 P_{1k}$ for the settings set in the model's PPR to be calculated with Eqs. (3) and (4) (see Appendix D). With only four data points available in the PPR, the $1/t^\circ - P_1$ plot appears to be a straight line, validating Eqs. (3) and (4) (Figure 3F). By Eqs. (9a) and (9b), $W^\circ \approx 11,774$ J (≈ 1.13 A·h) and $P_{00} \approx 1059$ J/yr (33.6 μ W). These estimates of W° and P_{00} allow the longevity of Quadra Assura MP to be projected for the settings in the Viva Quad XT manual (see Appendix D, Figure 3F).

Similar results were obtained from the pacing power analyses on the Platinum 4LV SonR (Figure 4; Appendix E). The LR in Platinum 4LV SonR has finer V_C increments (1 V instead of 2.5 V) and double the number of line/curve segments than the Quadra Assura MP.

3.3 | Shock therapy power

The data available only allowed shock therapy power analyses on three device models (Table 4).

For the Resonate X4, the $1/t^\circ - f_s$ plot for VVI(R) with 0% RV pacing comprises two straight lines of different slopes intersecting at $f_s = 4$ (Figure 5A). The $1/t^\circ - V_1^2$ plots (100% RV pacing at 0.4 ms and 500 Ω) for $f_s = 0, 4,$ and 8 are three parallel lines with the same slope but different $1/t^\circ$ -intercepts (Figure 5B). The estimated shock energy efficiency η_s is ≈ 1.5 for $f_s \leq 4$ and ≈ 0.75 for $f_s > 4$ (Table 4).

For the Platinum 4LV SonR, the $1/t^\circ - f_s$ plot for VVI 100% biventricular (BiV) pacing comprises straight lines of different slopes intersecting at $f_s = 2$ (Figure 5C). The $1/t^\circ - P_{12}$ (LV pacing power) plots (for 100% BiV pacing, RV amplitude 2.5 V at 0.35 ms and 500 Ω) for $f_s = 0, 2,$ and 4 are three parallel lines with the same slope but different $1/t^\circ$ -intercepts (Figure 5D). The estimated shock energy efficiency η_s is ≈ 2.4 for $f_s < 2$ and ≈ 0.45 for $f_s \geq 2$ (Table 4).

For the Intica 7 HF-T (QP), the only data available for the study were two tables in the device's manual showing how combinations of percentage of triple chamber pacing $\%_p$ (2.5 V, 0.4 ms, 500 Ω) and shock frequency f_s affect longevity. The table for no multipoint LV pacing was

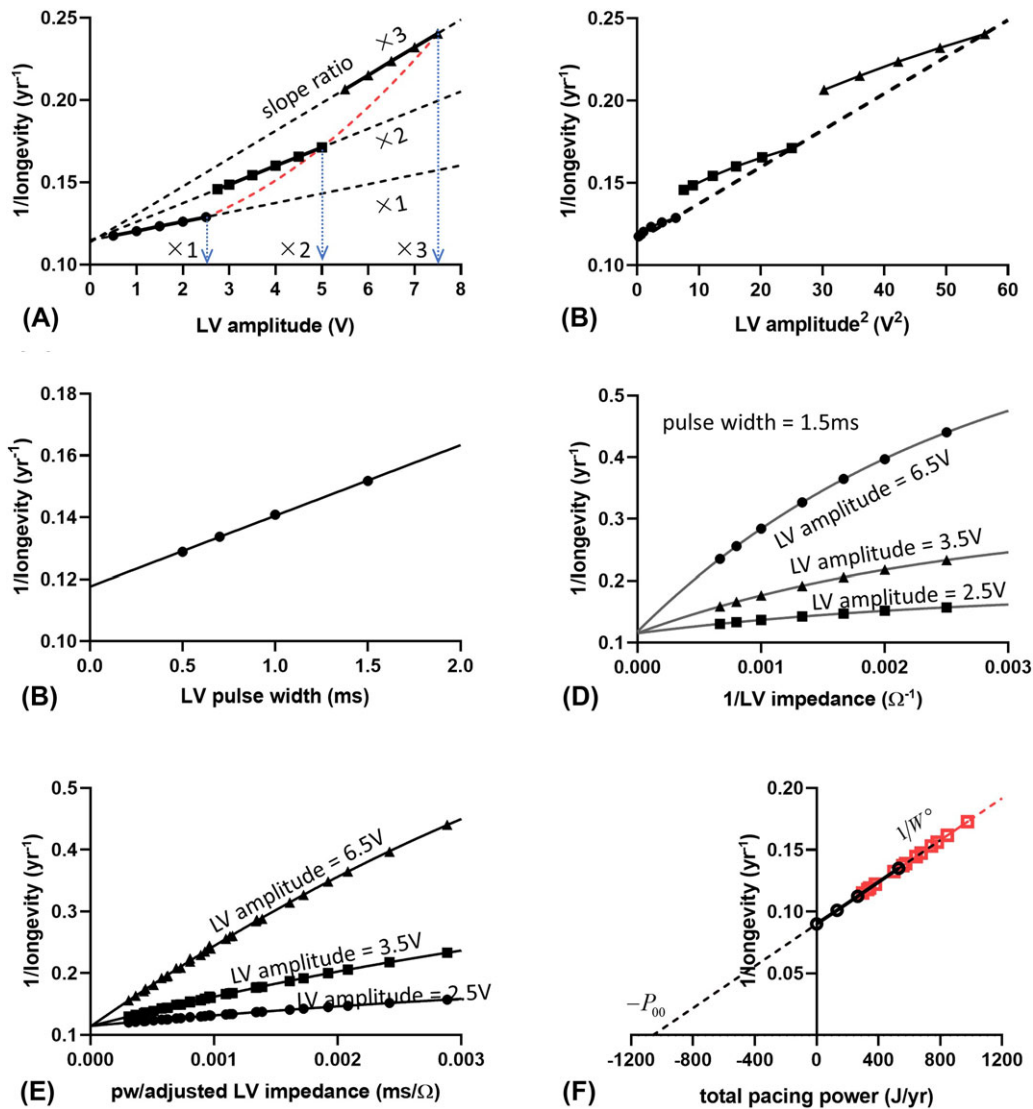


FIGURE 3 Effects of LV pacing amplitude, pulse width (pw), and impedance (with or without adjustment for internal resistance) on the longevity of the Quadra Assura MP CRT-D. The parameters of pacing were altered from the default values of 2.5 V, 0.5 ms, and 500 Ω . (A) The plot of the reciprocal of longevity against LV amplitude comprises three rising steepening straight line segments separated by widening abrupt jumps. The line segments have a common vertical intercept and slopes proportional to the LV amplitude at their upper ends, which lie on a parabola. (B) The plot of the reciprocal of longevity against the square of LV amplitude comprises three rising flattening convex curve segments separated by widening abrupt jumps and whose upper ends lie on a straight line. (C) The reciprocal of longevity is linearly related to the LV pw. (D) The plots of the reciprocal of longevity against the reciprocal of LV impedance are a series of convex upward curves with curvature positively with the LV amplitude. (E) The plots of the reciprocal of longevity against the pw: adjusted LV impedance (with the addition of an estimated internal resistance) are still a series of convex upward curves, but have many more data points on each due to the larger number of combinations of pw and adjusted LV impedance pairs. Modeling these curves as parabolas allows capacitance to be estimated. (F) The plot of the reciprocal of longevity against the calculated total pacing power is a straight line for the four data points available in the model's performance report (black circles). The slope of the line is the reciprocal of the usable battery energy $1/W^0$. The horizontal intercept is the negative value of the background power P_{00} . These two values allow the longevity of the Quadra Assura MP to be estimated for the same pacing settings chosen for the settings in the Viva Quad XT manual (red circles). CRT-D = cardiac resynchronization therapy defibrillator; LV = left ventricular; pw = pulse width [Color figure can be viewed at wileyonlinelibrary.com]

used (see Appendix F). The $1/t^0 - f_s$ plots for different $\%_p$'s (Figure 5E) and $1/t^0 - \%_p$ plots for different f_s 's (Figure 5E) are parallel lines. The lowest $f_s = 4$ because the device performs four high voltage capacitor reformations each year even if no shock therapy is delivered. The plot for $f_s = 16$ appears to be an outlier and the corresponding data were excluded for regression analysis (Figure 5F). The estimated shock energy efficiency is ≈ 0.84 for $f_s \geq 4$ (Table 4).

3.4 | Pacing modes, paced ventricular chambers, and other nonessential functions

The powers (measured with $\Delta(1/t^0)$) consumed by different combinations of binary functions with 0% pacing and 0 shocks for the Resonate X4 estimated with the BSc online longevity calculator are summarized in Table 5. Even with no actual pacing delivered, the dual-chamber

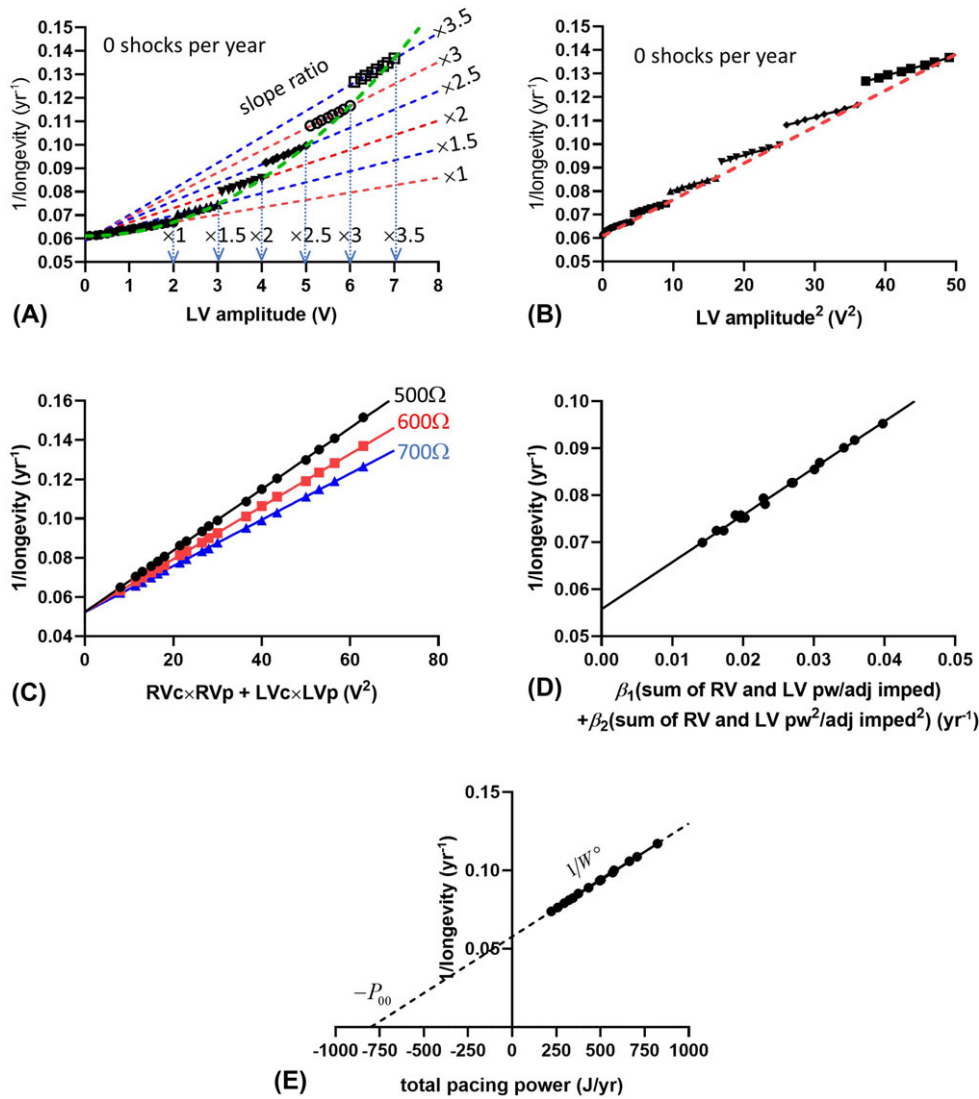


FIGURE 4 Plots of the reciprocal of longevity against pacing parameters or their derivatives for the Platinum 4LV SonR CRT-D. β_1 and β_2 = regression coefficients; CRT-D = cardiac resynchronization therapy defibrillator; LV = left ventricle; LVc = LV pacing capacitor peak voltage; LVp = LV pacing amplitude; P00: background power; pw = pulse width; RV = right ventricle; RVc = RV pacing capacitor peak voltage; RVp = RV pacing amplitude; W° = usable battery energy (see the main text and Appendix E for details) [Color figure can be viewed at wileyonlinelibrary.com]

pacing modes (DDD(R) and DDI(R)) consume 60% more power than VVI(R), which in turn consumes 20% more power than AAI(R). Maintaining readiness for RV-only and LV-only pacing consumes the same power, and less than for BiV pacing (see Appendix A). Maintaining readiness for multisite pacing and remote monitoring consume 1/3 and 2/3 the power of VVI(R). The heart failure sensor suite consumes 20% of the power consumed by remote monitoring. One of the first four shocks in a year consumes \approx 20% of the energy consumed by 100% pacing at 2.5 V, 0.4 ms, and 500 Ω .

The combination of VVI(R) with no ventricular chamber ($P_{31} + P_{40}$) is not available on the BSc online longevity calculator for the Resonate X4. Assuming VVI(R) consumes the same power as AAI(R) (i.e., $P_{31} = P_{32}$) and $P_{40} = 0$, then maintaining readiness for RV pacing consumes 0.001 in $\Delta(1/t^\circ)$ (i.e., $P_{41} = (P_{31} + P_{41}) - (P_{32} + P_{40})$, Table 5). This allows figures to be assigned to all the programmable states in Table 2. (Similar analyses were also possible for the Platinum 4LV SonR but they were not performed.)

3.5 | Longevity projection simulation

The longevity projections for the Resonate X4 by the mathematical model in Eq. (7) and estimates in Table 2 for various settings were compared with those by the BSc online longevity calculator (Table 6).

3.6 | Comparison of CRT-D models

For the Viva Quad XT, the only source of longevity data available to the study was its manual. Based on a previous publication,¹⁵ pacing appears to be powered by LR with transition at $V_p = 2.5, 3.5, 5, 7.5,$ and 8 V. Assuming internal resistance $\alpha_p = 100 \Omega$, pacing capacitance $C_p = 0.01$ mF, and pacing energy efficiency $\eta_p = 0.85$ for all channels, the total pacing power P_1 according to the settings in its manual was calculated (see Appendix G). The $1/t^\circ - P_1$ plot comprises two lines with the same $1/t^\circ$ intercept but different slopes (ratio 1.08; LV amplitude = 4 V for all the points on the less steep line; Figure 6A).

TABLE 4 Estimation of shock energy efficiency by two different methods for three different CRT-D models

(a) Impact of shock frequency on longevity										
Device	Resonate X4		Platinum 4LV SonR		Intica 7 HF-T (QP)					
	Shocks per year		Shocks per year		% triple chamber pacing					
Groups	0 – 4	4 – 10	0 – 2	2 – 4	0	15	50	100		
Slope $W_s/\eta_s W^\circ$	0.00216	0.004374	0.001184	0.006809	0.005132	0.005117	0.005081	0.005159		
$1/t^\circ$ -Intercept y_0	0.05849	0.04984	0.07576	0.06444	0.07791	0.08567	0.102	0.1246		
Usable battery energy W° (J)	13410	13290	13583	13610	9500	9500	9500	9500		
Shock energy W_s (J)	41	41	42	42	41	41	41	41		
Shock energy efficiency η_s	1.42	0.71	2.61	0.45	0.84	0.84	0.85	0.84		
(b) Equivalence between shock and pacing powers										
Device	Resonate X4 (Figure 4B)			Platinum 4LV SonR (Figure 4D)			Intica 7 HF-T (QP) (Figure 4F)			
	0	4	8	0	2	4	4	8	12	20
Slope	0.00172	0.00174	0.00176	0.000074	0.000074	0.000073	0.00011	0.00011	0.00011	0.00010
$1/t^\circ$ -intercept y_0	0.05775	0.06652	0.08405	0.06405	0.06663	0.08008	0.09922	0.1192	0.1398	0.1817
x-intercept x_0	-33.55	-38.3	-47.74	-869.9	-906.3	-1091	-939.7	-1088	-1314	-1734
Scale factor λ	23.09	23.09	23.09	1	1	1	1	1	1	1
Usable battery energy W° (J)	13410	13290	13112	13583	13602	13619	9471	9123	9403	9541
Background power P_{00} (J/yr)	775	884	1102	870	906	1091	940	1088	1314	1734
Δx_0		4.75	9.44		36	185		148.3	226	420
$\Delta P_p = \lambda \cdot \Delta x_0$ (J/yr)		110	218		36	185		148.3	226	420
Δf_s (spyr)		4	4		2	2		4	4	8
Shock energy W_s (J)		41	41		42	42		41	41	41
Shock energy efficiency η_s		1.5	0.75		2.31	0.45		1.11	0.73	0.78

Note: Usable battery energy W° estimated from linear regression of the corresponding pacing power in Table 4(b). CRT-D = cardiac resynchronization therapy defibrillator.

Postulating the LV channel was more energy efficient for output amplitude > 3.5 V, η_p was set to 0.8 for A/RV/LV amplitude ≤ 3.5 V and 0.9 for LV amplitude > 3.5 V and that aligns the two lines (see Appendix G; Figure 6B). The estimated usable battery energy W° is 6932 J (≈ 0.66 A·h) and the background power P_{00} 696 J/yr (22.1 μ W) for the Viva Quad XT. The total pacing powers of other CRT-D models for the Viva Quad XT settings were calculated and plotted against longevity projected by either the manufacturers (BSc, Mcp) or Eq. (7) (Abt, Btk) (Table 7, Figure 6B).

4 | DISCUSSION

Longevity projections reported in publicly available sources are for settings chosen by the manufacturers. For particular settings, users generally need to request the longevity estimates specifically from the manufacturers. The situation changed when BSc launched its online longevity calculator. For the first time in CIED history, users can freely “experiment” with the possible combinations of device settings and independently assess their impact on device longevity. The input and output data of these “experiments” allow inferences to be drawn on the structure and functions of CIEDs and they can have implications for clinical practice. The BSc and Mcp online longevity calculator and simulator are different from the Mdt online longevity calculator, which estimates the remaining longevity based on the previous clinical use

experience (the implantation date and the battery voltage at a subsequent date) and does not allow the user to alter the device settings.

4.1 | Validity of the mathematical model

The equations in the article and Appendices A and B are derived from fundamental principles of electric energy with some basic assumptions about the structure and operation of the CIED. The mathematical model explains, agrees with (especially Figures 2F and 6B), and predicts (Table 6) the impact on longevity by pacing, shock therapy, and other functions (either individually or in combination), proving its validity.

4.2 | Power supply for pacing

If SR is used to power pacing, the $1/t^\circ - V_p$ plot is a parabola and the $1/t^\circ - V_p^2$ plot is a straight line (Figures 1C and D). If LR is used, the $1/t^\circ - V_p$ plot comprises rising steepening straight line segments separated by widening abrupt jumps and whose upper ends lie on a parabola (Figures 3A and 4A), and the $1/t^\circ - V_p^2$ plot comprises rising flattening convex curve segments separated by widening abrupt jumps and whose upper ends lie on a straight line (Figures 3B and 4B). The straight line segments of $1/t^\circ - V_p$ plot share a common $1/t^\circ$ intercept (constant background power) and have slopes proportional to the V_p values at their upper ends (Figures 3A and 4A).

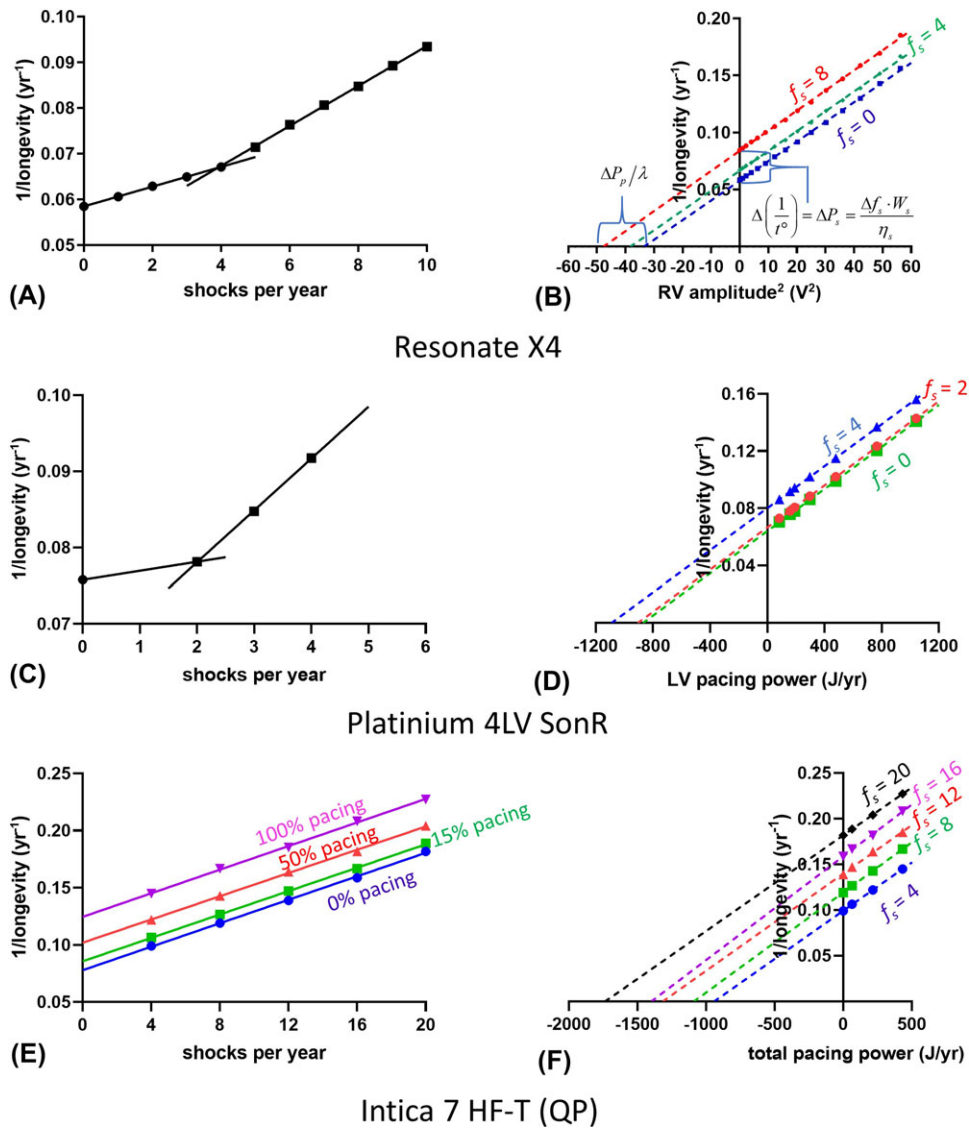


FIGURE 5 Effects of shock therapy frequency on CRT-D longevity. (A), (C), (E) The plot of the reciprocal of longevity $1/t^\circ$ against shock frequency f_s comprises straight lines. For Resonate X4 and Platinum 4LV SonR, the slope of the plot changes abruptly at $f_s = 4$ and 2 spyr, respectively. (B) For Resonate X4, a higher f_s shifts the plot of $1/t^\circ$ against the square of RV amplitude upwards parallelly. The change $\Delta(1/t^\circ)$ is larger for $\Delta f_s = 8 - 4$ than for $\Delta f_s = 4 - 0$. (D) For Platinum 4LV SonR, a higher f_s shifts the plot of $1/t^\circ$ against LV pacing power upwards parallelly. The change $\Delta(1/t^\circ)$ is larger for $\Delta f_s = 4 - 2$ than for $\Delta f_s = 2 - 0$. (F) For Intica 7 HF-T (QP), the plots of $1/t^\circ$ against the total pacing power for different values of f_s are roughly parallel. The line for $f_s = 16$ appears to be an outlier. LV = left ventricular; RV = right ventricular [Color figure can be viewed at wileyonlinelibrary.com]

The deviation of the $1/t^\circ - V_p$ and $1/t^\circ - V_p^2$ plots from the parabola and straight line “backbones” represents the theoretical energy inefficiency of LR compared to SR. The energy inefficiency increases with each successive jump (becomes wider) and diminishes when the pacing amplitude V_p approaches the peak pacing capacitor voltage V_C . Even though SR may be more energy efficient than liner regulation for pacing, it has its disadvantages (e.g., generation of electromagnetic noise from switching, vulnerability to electromagnetic inference during magnetic resonance imaging, see Appendix A) and the pacing energy efficiency advantage decreases if LR is implemented with finer increments for V_C (e.g., 1 V instead of 2.5 V, compare Figures 4A/b with Figures 3A/B). The different types of voltage regulation are not mutually exclusive and can be used in conjunction (see Appendices A and E).

4.3 | Shock energy efficiency

Manufacturers may quote several shocks per year in the publicized materials on the longevity of their ICD and CRT-D models, but it is not always clear whether these shocks include the periodic high-energy discharges for high-voltage capacitor reformation or battery conditioning. For the Resonate X4 and Platinum 4LV SonR, energy of the first four and two shocks in a year may be offset against the energy included in the background power consumption for high-voltage capacitor reformation/battery conditioning, leading to an apparent shock energy efficiency > 1 (Table 4) and lower than expected rises in background power when pacing power is modified by shock frequency (Figures 5B and D). Battery conditioning may consume less energy than

TABLE 5 Powers consumed by functions (components) of the Resonate X4 CRT-D

State	Code	t°	$1/t^\circ$	Pacing mode	$\Delta(1/t^\circ)$	V chamber	$\Delta(1/t^\circ)$	Others	$\Delta(1/t^\circ)$
OOO+no V	$P_0+P_{30}+P_{40}^*$	18.5	0.054054						
VVIR+RV	$P_0+P_{31}+P_{41}$	17	0.058824	(VVIR+RV)-(OOO+no V)	0.0047695				
VVIR+BiV	$P_0+P_{31}+P_{42}$	16.3	0.06135			BiV-RV	0.002526		
VVIR+LV	$P_0+P_{31}+P_{43}$	17.1	0.05848			BiV-LV	0.00287		
AAIR+no V	$P_0+P_{32}+P_{40}^*$	17.3	0.057803	(VVIR+RV)-(AAIR+no V)	0.0010201				
VDDR+RV	$P_0+P_{33}+P_{41}$	16.5	0.060606	VDDR-VVIR	0.0017825				
VDDR+BiV	$P_0+P_{33}+P_{42}$	15.7	0.063694	VDDR-VVIR	0.0023446	BiV-RV	0.003088		
VDDR+LV	$P_0+P_{33}+P_{43}$	16.5	0.060606	VDDR-VVIR	0.0021265	BiV-LV	0.003088		
DDIR+RV	$P_0+P_{34}+P_{41}$	16.3	0.06135	DDIR-VVIR	0.0025262				
DDIR+BiV	$P_0+P_{34}+P_{42}$	15.5	0.064516	DDIR-VVIR	0.0031664	BiV-RV	0.003166		
DDIR+LV	$P_0+P_{34}+P_{43}$	16.3	0.06135	DDIR-VVIR	0.0028702	BiV-LV	0.003166		
DDDR+RV	$P_0+P_{35}+P_{41}$	16.2	0.061728	DDDR-VVIR	0.0029049				
DDDR+BiV	$P_0+P_{35}+P_{42}$	15.5	0.064516	DDDR-VVIR	0.0031664	BiV-RV	0.002788		
DDDR+LV	$P_0+P_{35}+P_{43}$	16.2	0.061728	DDDR-VVIR	0.0032489	BiV-LV	0.002788		
VVIR+BiV+MSP	$P_0+P_{31}+P_{42}+P_5$	15.9	0.062893					MSP	0.0015434
VVIR+LV+MSP	$P_0+P_{31}+P_{43}+P_5$	16.7	0.05988			BiV-LV	0.003013	MSP	0.0014007
VDDR+BiV+MSP	$P_0+P_{33}+P_{42}+P_5$	15.4	0.064935	VDDR-VVIR	0.002042			MSP	0.0012408
VDDR+LV+MSP	$P_0+P_{33}+P_{43}+P_5$	16.2	0.061728	VDDR-VVIR	0.0018482	BiV-LV	0.003207	MSP	0.0011223
DDIR+BiV+MSP	$P_0+P_{34}+P_{42}+P_5$	15.2	0.065789	DDIR-VVIR	0.0028964			MSP	0.0012733
DDIR+LV+MSP	$P_0+P_{34}+P_{43}+P_5$	15.9	0.062893	DDIR-VVIR	0.0030128	BiV-LV	0.002896	MSP	0.0015434
DDDR+BiV+MSP	$P_0+P_{35}+P_{42}+P_5$	15.2	0.065789	DDDR-VVIR	0.0028964			MSP	0.0012733
DDDR+LV+MSP	$P_0+P_{35}+P_{43}+P_5$	15.9	0.062893	DDDR-VVIR	0.0030128	BiV-LV	0.002896	MSP	0.0011647
OOO+no V+RM	$P_0+P_{30}+P_{40}+P_6$	17.4	0.057471					RM	0.0034172
VVIR+RV+RM	$P_0+P_{31}+P_{41}+P_6$	16.1	0.062112	(VVIR+RV)-(OOO+no V)	0.0046405			RM	0.0032883
AAIR+no V+RM	$P_0+P_{32}+P_{40}+P_6$	16.3	0.06135	AAIR-OOO	0.0038784			RM	0.0035462
OOO+no V+MV	$P_0+P_{30}+P_{40}+P_7$	17.5	0.057143					MV	0.0030888
VVIR+RV+MV	$P_0+P_{31}+P_{41}+P_7$	16.3	0.06135	(VVIR+RV)-(OOO+no V)	0.0042068			MV	0.0025262
AAIR+no V+MV	$P_0+P_{32}+P_{40}+P_6$	16.4	0.060976	AAIR-OOO	0.0038328			MV	0.0031721
OOO+no V+HFS	$P_0+P_{30}+P_{40}+P_8$	18.2	0.054945					HFS	0.000891
VVIR+RV+HFS	$P_0+P_{31}+P_{41}+P_8$	16.9	0.059172	(VVIR+RV)-(OOO+no V)	0.0042265			HFS	0.0003481
AAIR+no V+HFS	$P_0+P_{32}+P_{40}+P_8$	17.1	0.05848	AAIR-OOO	0.0035345			HFS	0.0006761
OOO+1 spyr	$P_0+P_{30}+P_{40}+1 \text{ spyr}$	17.8	0.05618					1 spyr	0.0021257
VVIR+RV+ < P_p >	$P_0+P_{31}+P_{41}+ < P_p >$	14.6	0.068493					< P_p >	0.0096696

Note: 0% atrial and ventricular pacing and 0 shocks generally assumed; t° = device longevity; $\Delta(1/t^\circ)$ difference in reciprocal of device longevity; $\langle P_p \rangle$ = power of 100 % RV pacing at 2.5 V at 0.4 ms and 500 Ω ; BiV = biventricular; CRT-D = cardiac resynchronization therapy defibrillator; HFS = heart failure suite; LV = left ventricular; MSP = multi-site pacing; MV = minute ventilation; RM = remote monitoring; RV = right ventricular; spyr = shocks per year.

a maximum therapeutic shock for a device (e.g., 34 J vs 42J the Platinum 4LV SonR).

Beyond energy offsetting, the estimated shock energy efficiency is 0.45, 0.75, and 0.85 (Table 4). The shock energy efficiency of 0.45 is not necessarily due to bad engineering, but may reflect a conscious decision to maximize power transfer (shorten charge time) during shock therapy. By the maximum power theorem, power transfer from a battery is maximum when energy efficiency is 0.5.^{15,16}

4.4 | Longevity, usable battery energy, background power, and pacing power supply

Clinical discussion on device longevity has often focused on battery capacity (usable battery energy W°)^{17,18} and neglected background power P_{00} and pacing power supply. Figure 6B provides a graphical illustration of the interplay of the three factors. The $1/t^\circ - P_1$ (total pacing power) plot is entirely determined by the horizontal intercept

TABLE 6 Comparison of longevity projections by mathematical model and online calculator for the Resonate X4 CRT-D

Programmable states (setting)	Power (1/t°)	DDD + 15% A pacing + 100% RV-only pacing	DDD + 50% A pacing + 50% RV-only pacing + 2 shocks per year	DDD + 20% A pacing + 80% RV-only pacing + 6 shocks per year	DDD + 20% A pacing + 90% RV-pacing + 90% LV pacing@2.5V	DDD + 15% A pacing + 70% LV only pacing @3V + 70% MSP LVb pacing@4V	DDD + 25% A pacing + 80% RV pacing + 90% LV pacing@3.5V + 90% MSP LVb@4.5V + 8 shocks per year + RM
P0	0.058	0.058	0.058	0.058	0.058	0.058	0.058
P10	0.0097	0.001455	0.00485	0.00194	0.00194	0.00194	0.002425
P11	0.0097	0.0097	0.00485	0.00776	0.00873	0	0.00776
P12	0.0097	0	0	0	0.00873	0.009778	0.017111
P13	0.0097	0	0	0	0	0.017382	0.028285
P2 (fs ≤ 4)	0.0021	0	0.0042	0.0084	0	0	0.0084
P2 (fs > 4)	0.0042	0	0	0.0084	0	0	0.0168
P30	0	0	0	0	0	0	0
P31	0.0037	0	0	0	0	0	0
P32	0.0037	0	0	0	0	0	0
P33	0.0057	0	0	0	0	0	0
P34	0.0065	0	0	0	0	0	0
P35	0.0067	0.0067	0.0067	0.0067	0.0067	0.0067	0.0067
P40	0	0	0	0	0	0	0
P41	0.001	0.001	0.001	0.001	0	0	0
P42	0.004	0	0	0	0.004	0	0.004
P43	0.001	0	0	0	0	0.001	0
P5	0.0012	0	0	0	0	0.0012	0.0012
P6	0.0033	0	0	0	0	0	0.0033
P7	0.003	0	0	0	0	0	0
P8	0.0006	0	0	0	0	0	0
Sum(1/t°)		0.076855	0.0796	0.0922	0.0881	0.096	0.153981
Longevity		13.0	12.6	10.8	11.4	10.4	6.5
Online calculator		13.7	13.1	11.2	11.7	10.7	6.4

Note: fs = shock frequency; CRT-D = cardiac resynchronization therapy defibrillator; MSP = multisite pacing; RM = remote monitoring; RV = right ventricular.

TABLE 7 Projected longevity for five CRT-D models standardized to the settings in the Viva Quad XT manual

	15	15	15	15	15	15	15	15	15	15	15	15	15	15	15	15
% A pacing																
A amplitude (V)	2	2	2.5	2.5	2.5	3.5	3.5	2	2	2.5	2.5	2.5	3.5	3.5		
% RV pacing	100	100	100	100	100	100	100	100	100	100	100	100	100	100	100	100
RV amplitude (V)	2	2	2.5	2.5	2.5	3.5	3.5	2	2	2.5	2.5	2.5	3.5	3.5		
% LV pacing	100	100	100	100	100	100	100	100	100	100	100	100	100	100	100	100
LV amplitude (V)	2.5	4	2.5	3	4	2.5	4	2.5	4	2.5	3	4	2.5	4		
Impedance (ohm)	500	500	500	500	500	500	500	600	600	600	600	600	600	600	600	600
	Usable battery energy	Background power	Longevity													
Platinum 4LV SonR	13843 J (≈ 1.33 A·h)	799 J/yr (25.3 μW)	13.1	10.0	12.1	11.7	9.4	10.6	8.5	13.5	10.7	12.6	12.3	10.1	11.2	9.2
Resonate X4	13619 J (≈ 1.30 A·h)	918 J/yr (29.1 μW)	11.6	9.8	11.1	10.5	9.4	9.8	8.4	12	10.2	11.5	11	9.9	10.3	9
Quadra Assura MP	11774 J (≈ 1.13 A·h)	1059 J/yr (33.6 μW)	8.4	6.5	8.2	6.9	6.4	7.2	5.8	8.7	6.9	8.5	7.3	6.8	7.6	6.2
Intica 7 HF-T (QP)	9471 J (≈ 0.907 A·h)	940 J/yr (29.8 μW)	7.8	6.1	7.6	6.5	6	6.7	5.5	8	6.5	7.8	6.8	6.4	7	5.8
Viva Quad XT	6932 J (≈ 0.664 A·h)	696 J/yr (22.1 μW)	7	5.4	6.8	6.1	5.3	5.8	4.7	7.3	5.8	7.1	6.4	5.6	6.1	5

Note: Base rate: 60 beats/min. Pulse width: 0.35 ms (Platinum 4LV SonR); 0.4 ms (Resonate X4; Intica 7 HF-T(QP); Viva Quad XT); 0.5 ms (Quadra Assura MP). CRT-D = cardiac resynchronization therapy defibrillator; LV = left ventricular; RV = right ventricular.

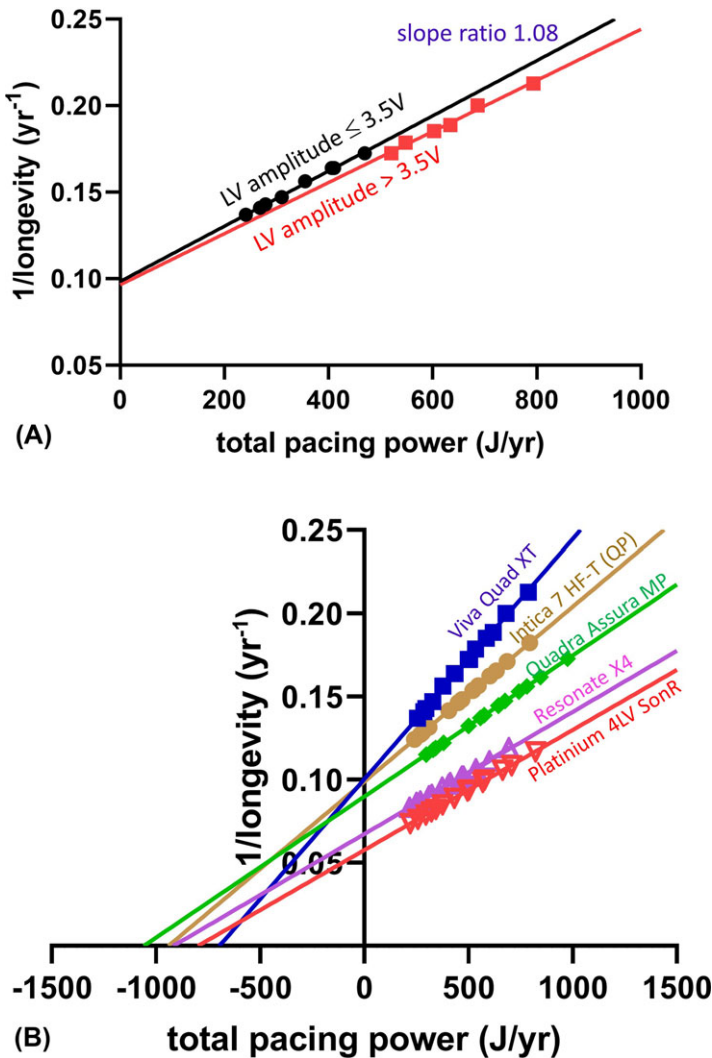


FIGURE 6 Effect on longevity by the calculated total pacing power for the Viva Quad XT and other cardiac resynchronization therapy defibrillator models for the same settings [Color figure can be viewed at wileyonlinelibrary.com]

$-P_{00}$, slope $1/W^\circ$, and variable P_1 (Eq. (8)). The Platinum 4LV SonR has the highest calculated W° (most gentle slope) and lowest calculated P_{00} (least negative horizontal intercept) among all the CRT-D models examined (Table 7, Figure 6B) based on longevity projection data provided by manufacturers. A low background power (which may require switching off certain standard functions such as pre-arrhythmia electrogram storage) can partially but not completely compensate for a low usable battery energy in extending device longevity, especially when the clinical need for and power consumed by therapy is high. LR with fine increments (e.g., Platinum 4LV SonR) is more energy efficient (tighter clustering and downward migration of data points for the same pacing settings) than with large increments (e.g., Quadra Assura MP) and can approach SR (e.g., Resonate X4) in pacing energy efficiency. Pacing can constitute a large part of the power consumption for a CIED (especially a CRT-D). The patient's clinical needs for pacing cannot always be anticipated or controlled. SR or LR with fine increments will help keep P_1 low for the same pacing settings.

The usable battery energy W° for the Resonate X4 was estimated to be $\approx 1.3\text{--}1.4\text{ A}\cdot\text{h}$ (Table 3). The EnduraLife battery is claimed by its manufacturer BSc to have a total capacity of $1.9\text{ A}\cdot\text{h}$ for the Resonate X4, which means $\approx 74\%$ ($= 1.4/1.9$) of the battery's energy store is usable.

4.5 | Dormant activated functions or components

The logical circuits for regulating pacing need to run continuously, even if no pacing is actually delivered. The more chambers are sensed and paced, the more steps are in the logical circuits, and the more power is consumed. In this light, for patients who are unlikely to require significant pacing support, it would be advisable to choose VVI(R) over DDD(R) even if the ICD is a dual chamber one in order to conserve energy. (The atrial channel can still be used for ventricular tachyarrhythmia diagnosis.) For the same pacing mode, reducing the number of paced chambers conserves energy (even if no pacing is actually delivered). To maximize device longevity, dormant nonessential functions should be switched off.

4.6 | Extended or shortened device longevity—whose credit and whose fault?

When a CIED lasts longer or shorter than expected, the manufacturer often takes the credit and the blame.^{17,19} How long a device lasts in clinic use depends on the: (1) usable battery energy, (2) the minimum operational power, (3) the therapies delivered, and (4) other activated non-essential functions. The first two items are controlled by the

manufacturer, but the two last items are determined by the patient's clinical needs and programming by healthcare professionals. Device therapies can consume more power than the background operations. Premature (significantly earlier than projected by the manufacturer) device failure due to battery depletion in clinical use is probably mostly driven by the patient's clinical needs for therapy, partially due to suboptimal programming by healthcare professionals, and unlikely to be the manufacturer's fault unless component failure can be clearly identified.^{20,21}

4.7 | Conclusions

Longevity has become a major focus of attention for a CIED's clinical performance, but is in fact a direct consequence of how quickly the powers consumed by the device's functions and components exhaust its finite usable battery energy store. A mathematical model for CIED power consumptions was derived from fundamental principles of electric energy and validated against longevity data from multiple manufacturers. Compared to longevity estimated for a single set of standardized settings,⁸ the methodology described in the article allows the user to make multiple longevity projections for clinically relevant settings freely without further input from manufacturers. The power consumed by pacing can be theoretically derived and used for estimating the background power, shock therapy energy efficiency, the powers consumed by other functions, and the usable battery energy of CIEDs. The powers consumed by therapy functions are dictated by the clinical needs of the patient, but healthcare professionals can reduce power consumption by switching off dormant functions and reducing the clinical needs for device therapies such as by catheter ablation of ventricular tachycardia.²²⁻²⁵ As power consumption of a device in clinical use may not be reliably anticipated or modified, the surest way to extend a device's duration in service is to implant a model with a large usable battery energy, a low background power, and energy efficient pacing and shock therapy.

5 | LIMITATIONS

Because longevity is typically expressed in years to one decimal point, and regression analysis is done on its reciprocal, the regression parameters may be subjected to error and instability, especially when power consumption is high and longevity is low. The mathematical model described in this article tries to "reverse-engineer" the mathematical models used by manufacturers to project the longevity of their products rather than predict their actual service lifespan in clinical use. The mathematical model fits the data from the BSc online longevity calculator remarkably well, but may not accurately reflect how the calculator is programmed by the manufacturer. The inferences drawn from the mathematical model on device construction and function cannot be verified. Lead insulation breach can lower pacing impedance drastically and invalidate the approximations in Eqs. (2) and (3) (and Eqs. (B3) and (B4) in Appendix B). A single clinical shock defers the next high-voltage capacitor reformation/battery conditioning by the same duration as multiple shocks in quick succession, making it hard to offset shock therapy against high-voltage capacitor reformation/battery conditioning in

longevity projection. Equations (6), (7), (10), and (11) assume all shocks are at the same (maximum) output, which may be not true in clinical practice. The methodology described in this study permits the user more freedom in choosing the settings for longevity projection, but still requires a minimum ("training") set of data from the manufacturers to implement. Manufacturers make disparate assumptions about storage time before implantation, amount of radiofrequency communication during implantation, and frequency of remote monitoring in their longevity projections.

CONFLICTS OF INTEREST

EWL: consultancy (Abbott).

ACKNOWLEDGMENTS

The author thanks Hal Propp and William Linder from Boston Scientific, Daniel Kroiss and Jean-Renaud Billuart from Microport, an Avi Fischer, Paul Ryu, and Matt Desmond from Abbott for helpful comments.

ORCID

Ernest W. Lau MD  <https://orcid.org/0000-0003-0030-9326>

REFERENCES

- Zanon F, Martignani C, Ammendola E, et al. Device longevity in a contemporary cohort of ICD/CRT-D patients undergoing device replacement. *J Cardiovasc Electrophysiol*. 2016;27:840-845.
- Boriani G, Braunschweig F, Deharo JC, Leyva F, Lubinski A, Lazzaro C. Impact of extending device longevity on the long-term costs of implantable cardioverter-defibrillator therapy: A modelling study with a 15-year time horizon. *Europace*. 2013;15:1453-1462.
- Poole JE, Gleva MJ, Mela T, et al. Complication rates associated with pacemaker or implantable cardioverter-defibrillator generator replacements and upgrade procedures: Results from the REPLACE registry. *Circulation*. 2010;122:1553-1561.
- Uslan DZ, Gleva MJ, Warren DK, et al. Cardiovascular implantable electronic device replacement infections and prevention: Results from the REPLACE Registry. *Pacing Clin Electrophysiol*. 2012;35:81-87.
- Nichols CI, Vose JG, Mittal S. Incidence and costs related to lead damage occurring within the first year after a cardiac implantable electronic device replacement procedure. *J Am Heart Assoc*. 2016;5:e002813.
- Borleffs CJ, Thijssen J, de Bie MK, et al. Recurrent implantable cardioverter-defibrillator replacement is associated with an increasing risk of pocket-related complications. *Pacing Clin Electrophysiol*. 2010;33:1013-1019.
- Boriani G, Ritter P, Biffi M, et al. Battery drain in daily practice and medium-term projections on longevity of cardioverter-defibrillators: An analysis from a remote monitoring database. *Europace*. 2016;18:1366-1373.
- Munawar DA, Mahajan R, Linz D, et al. Predicted longevity of contemporary cardiac implantable electronic devices: A call for industry-wide "standardized" reporting. *Heart Rhythm*. 2018;15:1756-1763.
- Schaer BA, Koller MT, Sticherling C, Altmann D, Joerg L, Osswald S. Longevity of implantable cardioverter-defibrillators, influencing factors, and comparison to industry-projected longevity. *Heart Rhythm*. 2009;6:1737-1743.

10. Shafat T, Baumfeld Y, Novack V, Konstantino Y, Amit G. Significant differences in the expected versus observed longevity of implantable cardioverter defibrillators (ICDs). *Clin Res Cardiol*. 2013;102:43-49.
11. Alam MB, Munir MB, Rattan R, Adelstein E, Jain S, Saba S. Battery longevity from cardiac resynchronization therapy defibrillators: Differences between manufacturers and discrepancies with published product performance reports. *Europace*. 2017;19:421-424.
12. Alam MB, Munir MB, Rattan R, et al. Battery longevity in cardiac resynchronization therapy implantable cardioverter defibrillators. *Europace*. 2014;16:246-251.
13. Landolina M, Curnis A, Morani G, et al. Longevity of implantable cardioverter-defibrillators for cardiac resynchronization therapy in current clinical practice: An analysis according to influencing factors, device generation, and manufacturer. *Europace*. 2015;17:1251-1258.
14. Lau EW. Leads and electrodes for cardiac implantable electronic devices. In: Ellenbogen KA, Wilkoff BL, Kay GN, Lau C-P, Auricchio A, eds. *Clinical Cardiac Pacing, Defibrillation, and Resynchronization Therapy*. 5th ed. Philadelphia: Elsevier; 2016:313-351.
15. Lau EW. Technologies for prolonging cardiac implantable electronic device longevity. *Pacing Clin Electrophysiol*. 2017;40:75-96.
16. Paul DK, Gardner P. Maximum power transfer theorem: A simplified approach. *Intl J Electrical Eng Educat*. 1998;35:271-273.
17. Evans JM, Cleves A, Morgan H, Millar L, Carolan-Rees G. ENDURALIFE-powered cardiac resynchronisation therapy defibrillator devices for treating heart failure: A NICE Medical Technology Guidance. *Appl Health Econ Health Policy*. 2018;16:177-186.
18. Ellis CR, Dickerman DI, Orton JM, et al. Ampere hour as a predictor of cardiac resynchronization defibrillator pulse generator battery longevity: A multicenter study. *Pacing Clin Electrophysiol*. 2016;39:658-668.
19. von Gunten S, Schaer BA, Yap SC, et al. Longevity of implantable cardioverter defibrillators: A comparison among manufacturers and over time. *Europace*. 2016;18:710-717.
20. Pokorney SD, Greenfield RA, Atwater BD, Daubert JP, Piccini JP. Novel mechanism of premature battery failure due to lithium cluster formation in implantable cardioverter-defibrillators. *Heart Rhythm*. 2014;11:2190-2195.
21. Hayashi Y, Takagi M, Kakihara J, Tatsumi H, Atsushi D, Yoshiyama M. A case of unexpected early battery depletion caused by lithium cluster formation in implantable cardioverter-defibrillator. *J Cardiol Cases*. 2017;15:184-186.
22. Acosta J, Cabanelas N, Penela D, et al. Long-term benefit of first-line peri-implantable cardioverter-defibrillator implant ventricular tachycardia-substrate ablation in secondary prevention patients. *Europace*. 2017;19:976-982.
23. Atti V, Vuddanda V, Turagam MK, et al. Prophylactic catheter ablation of ventricular tachycardia in ischemic cardiomyopathy: A systematic review and meta-analysis of randomized controlled trials. *J Interv Card Electrophysiol*. 2018;53:207-215.
24. Bunch TJ, Weiss JP, Crandall BG, et al. Patients treated with catheter ablation for ventricular tachycardia after an ICD shock have lower long-term rates of death and heart failure hospitalization than do patients treated with medical management only. *Heart Rhythm*. 2014;11:533-540.
25. Sapp JL, Wells GA, Parkash R, et al. Ventricular tachycardia ablation versus escalation of antiarrhythmic drugs. *N Engl J Med*. 2016;375:111-121.

SUPPORTING INFORMATION

Additional supporting information may be found online in the Supporting Information section at the end of the article.

How to cite this article: Lau EW. Longevity decoded: Insights from power consumption analyses into device construction and their clinical implications. *Pacing Clin Electrophysiol*. 2019;42:407-422. <https://doi.org/10.1111/pace.13642>